JOURNAL OF GEOPHYSICAL RESEARCH, VOL. 115, D08301, doi:10.1029/2009JD012675, 2010

Quantification of NO_2 and SO_2 emissions from the Houston Ship Channel and Texas City industrial areas during the 2006 Texas Air Quality Study

Claudia Rivera,[1] Johan Mellqvist,[1] Jerker Samuelsson,[1] Barry Lefer,[2] Sergio Alvarez,[3] and Monica R. Patel[2]

Received 16 June 2009; revised 21 November 2009; accepted 10 December 2009; published 23 April 2010.

[1] In August–September 2006, as part of the Second Texas Air Quality Study, NO_2 and SO_2 emissions from the Houston Ship Channel and Texas City industrial areas were quantified using mobile mini-differential optical absorption spectroscopy instruments. The measured NO_2 emissions from the Houston Ship Channel and Texas City industrial areas were 2542 and 452 kg h^{-1}, respectively, yielding NO_x emissions 70% and 43%, respectively, above the reported inventory values. Quantified SO_2 emissions from the Houston Ship Channel area were 1749 kg h^{-1} and were found to be 34% above the values reported in the inventory. Short-term variability of NO_2 and SO_2 emissions was found at the Houston Ship Channel. On 31 August 2006, a plume was detected at the HSC during three consecutive measurements, yielding a HCHO flux of 481 kg h^{-1}. This event has been mainly attributed to photochemical production.

Citation: Rivera, C., J. Mellqvist, J. Samuelsson, B. Lefer, S. Alvarez, and M. R. Patel (2010), Quantification of NO_2 and SO_2 emissions from the Houston Ship Channel and Texas City industrial areas during the 2006 Texas Air Quality Study, *J. Geophys. Res.*, *115*, D08301, doi:10.1029/2009JD012675.

1. Introduction

[2] Air pollution is a problem in many cities of the world, and the Houston-Galveston, Texas, area (HGA) is no exception, with one of the most severe ozone (O_3) problems in the United States. The process of tropospheric O_3 production by photochemical oxidation of industrial hydrocarbons involving NO and NO_2 as catalysts has been described in the literature [*Crutzen*, 1979]. This process is highly dependent on the concentration and chemical composition of hydrocarbons [*Grover and Bradford*, 2001], as well as on NO_x [*Jacob et al.*, 1996; *Kasibhatla et al.*, 1991; *Martin et al.*, 2002; *Murphy et al.*, 1993; *Penner et al.*, 1991]. Both NO_x and VOCs are a product of combustion processes, from either stationary or mobile sources, and have biogenic sources as well [*Conley et al.*, 2005; *Finlayson-Pitts and Pitts*, 2000]. In the HGA, emissions of these compounds are associated with petrochemical industrial facilities as well as traffic [*Berkowitz et al.*, 2005; *Buzcu-Guven and Fraser*, 2008; *De Gouw et al.*, 2009; *Gilman et al.*, 2009; *Jobson et al.*, 2004; *Leuchner and Rappenglück*, 2010; *Smith et al.*, 2007; *Xie and Berkowitz*, 2007].

[3] The Texas Air Quality Study 2000 (TexAQS 2000) demonstrated that industrial complexes in the HGA are large emitters of NO_x and hydrocarbons, which originate spatially localized plumes rich in O_3 and hydrocarbon oxidation products (i.e., formaldehyde) [*Daum et al.*, 2003, 2004; *Kleinman et al.*, 2002; *Ryerson et al.*, 2003]. Detailed studies have demonstrated that the high O_3 production rates in the HGA are linearly dependent on the ratio of total nonmethane hydrocarbons to NO_x [*Berkowitz et al.*, 2005]. In the HGA, the production tends to be more rapid and efficient than in other urban areas [*Kleinman et al.*, 2002; *Lei et al.*, 2004]. In addition a detailed particulate growth study in the HGA concluded that SO_2-rich plumes were associated with particle formation and substantial particle volume growth [*Brock et al.*, 2003].

[4] Formaldehyde has a very short lifetime (generally 2–4 h) in the presence of sunlight, which is determined mainly by photolysis and reaction with OH radicals [*Garcia et al.*, 2006; *Wert et al.*, 2003]. It can be directly emitted by incomplete combustion or industrial processes or be secondarily formed by oxidation of VOCs [*Finlayson-Pitts and Pitts*, 2000]. Studies have shown that oxidation of ethene, propene, and isoprene tends to efficiently produce HCHO [*Dodge*, 1990; *Goldan et al.*, 2000; *Lee et al.*, 1998; *Wert et al.*, 2003]. During TexAQS 2000, *Wert et al.* [2003] concluded that there was no evidence for strong primary emissions of HCHO when compared to the secondary emissions produced in several Houston area plumes.

[5] Worsening air quality in the HGA has increased the concern of the general public and policymakers regarding

[1]Radio and Space Science, Chalmers University of Technology, Gothenburg, Sweden.
[2]Department of Geosciences, University of Houston, Houston, Texas, USA.
[3]Institute for Air Science, Baylor University, Waco, Texas, USA.

0148-0227/10/2009JD012675

environmental problems generated by outdoor pollution and its relationship with human health [*Brody et al.*, 2004; *Conley et al.*, 2005]. Because O_3 threshold mixing ratios established by the National Ambient Air Quality Standard are frequently exceeded, the HGA has been designated an O_3 nonattainment region, and it is therefore important to identify and quantify O_3 precursors and reduce their emissions [*Allen et al.*, 2004; *Byun et al.*, 2007; *Grover and Bradford*, 2001; *Kleinman et al.*, 2002]. With the objective to provide detailed accurate emission information, a 5-week field campaign in the HGA was performed during the summer of 2006. NO_2, SO_2, and HCHO differential vertical columns were quantified in the Houston Ship Channel (HSC) and Texas City (TC) industrial areas by traversing the plume of these industrial complexes using a mini-differential optical absorption spectroscopy (DOAS) instrument installed on a car. The DOAS measurements of NO_2 and SO_2 presented here were conducted in parallel with airborne and mobile solar IR measurements to quantify VOC emissions [*De Gouw et al.*, 2009]. The latter study shows large discrepancies between measured and reported emissions. It was therefore of great interest to investigate whether discrepancies exist also for NO_2 and SO_2 emissions. The objective of this paper is to determine the consistency of our measurements with available emission inventories of the HGA.

2. Method and Data Analysis

[6] DOAS is a technique that allows the remote detection of trace gases. It is based on the absorption of electromagnetic radiation by matter and is widely used for continuously quantifying atmospheric gases [*Finlayson-Pitts and Pitts*, 2000; *Platt*, 1994; *Platt et al.*, 1979; *Platt and Stutz*, 2008]. DOAS measurements can be performed using a wide variety of experimental setups. In this field campaign, passive DOAS using scattered sunlight by air molecules and particles has been used in zenith scattered light configuration. Zenith scattered sunlight measurements offer a large variety of applications, are one of the earliest applications of passive DOAS, and have been used to study stratospheric chemistry and the radiative transport in clouds [*Platt and Stutz*, 2008].

2.1. Mobile Mini-Differential Optical Absorption Spectroscopy

[7] A mobile miniDOAS instrument, described in detail by *Galle et al.* [2002], was used to perform the measurements presented in this paper. MiniDOAS instruments have been widely adopted by the scientific community to quantify emissions from urban [*Johansson et al.*, 2008, 2009], industrial [*McGonigle et al.*, 2004; *Rivera et al.*, 2009], and volcanic [*Bobrowski et al.*, 2003; *Bobrowski and Platt*, 2007; *Galle et al.*, 2002; *Mori et al.*, 2006] sources. Our system utilizes an 8 mrad field of view telescope to collect scattered UV light. The telescope has a quartz lens and, only for SO_2 measurement purposes, a Hoya U-330 filter was used to reduce stray light, blocking visible light with wavelength higher than 360 nm. The telescope is then coupled to a 600 μm quartz fiber optic which transfers light into an Ocean Optics S2000 spectrometer with spectral resolution of approximately 0.6 nm and spectral range of 280–420 nm (SO_2 and HCHO) and 336–480 nm (NO_2). The spectrometer and a GPS were connected to a laptop computer controlled by custom-built software, Mobile DOAS [*Johansson and Zhang*, 2004], which acquired and preliminarily evaluated spectra in real time.

2.2. Measurement Method

[8] The mobile miniDOAS instrument was mounted on a car and aligned toward zenith, and spectra were recorded encircling the sources of pollution. Differential vertical columns of the species of interest were measured upwind and downwind of the sources in order to derive inflow and outflow, respectively, with the flux being the difference between them. For the Texas City industrial area, measurements were conducted traversing the downwind plume. Typically measurements were done 100 m to about 10 km (only the case of the HSC industrial area) downwind of the sources since these are distributed over large areas with no accessibility except for public roads. Every measurement series started with the recording of a background reference spectrum, considered to be the reference for all the following spectra recorded during the measurement series. Ideally the reference spectrum is expected not to include any concentration above ambient of the trace species of interest; however, in urban and industrial areas this is difficult to achieve, and therefore our measurement in this case will produce the difference in vertical columns between the background reference spectrum and all measured spectra across the plume for every measurement series. All vertical columns derived from spectra collected after the reference spectrum are relative to the latter and will be further referred to as differential vertical columns.

[9] It is important to notice that we have assumed that the light path is vertical and no air mass factor has been applied to the differential vertical columns, which could bring uncertainties to the results of our measurements. The measurements presented in this study were conducted during days of clear blue sky without presence of clouds. In order to give insight for high aerosol loads which could lead to enhanced light paths through multiple scattering, the oxygen dimer (O_4) was included into the DOAS fit. All measurements conducted during the field campaign that showed indication of enhanced light paths during the traverses were disregarded. More details about this procedure are given by *Johansson et al.* [2008]. In section 2.5, the uncertainty related to light path extension inside the plume (multiple scattering) as well as to scattering of photons into the instrument's field of view by particles beneath the plume (light dilution) is further discussed.

[10] Stratospheric NO_2 variations are expected to be small in the short time period (few minutes to 1 h) our measurements take when compared with tropospheric NO_2 variations present in the polluted plumes we are quantifying. In addition, using a background reference spectrum for each measurement series eliminates the stratospheric NO_2 part and has less influence of instrumental instabilities, as already pointed out by *Sinreich et al.* [2005].

[11] GPS data were recorded providing time and position before and after each spectrum was collected. Fluxes from traverses were calculated by multiplying differential total vertical columns by the distance traversed perpendicular to the wind direction and by the wind speed. Wind information

Table 1. Fitting Intervals and Molecules Included in the Differential Optical Absorption Spectroscopy Fit

Fitting Interval Wavelength Range (nm)	Species
310–325	SO_2, O_3, NO_2, HCHO, Ring
324–347	HCHO, O_3, NO_2, SO_2, O_4, Ring
420–460	NO_2, O_3, O_4, H_2O, Ring

was obtained from GPS sondes regularly launched during the field campaign (see section 2.4).

2.3. Spectral Evaluation

[12] SO_2, HCHO, and NO_2 were retrieved from the recorded spectra using the WinDOAS software (version 2.1) (*Van Roozendael and Fayt*, 2001) in the wavelength regions of 310–325, 324–347, and 420–460 nm, respectively. This procedure has been described in detail elsewhere [*Galle et al.*, 2002; *Platt and Stutz*, 2008]. The cross sections used in the DOAS fit (SO_2 [*Bogumil et al.*, 2003], HCHO [*Meller and Moortgat*, 2000], and NO_2 [*Vandaele et al.*, 1998]) were collected from the literature and degraded to our instrument's resolution. In addition, the cross sections of O_3 [*Voigt et al.*, 2001], O_4 [*Hermans et al.*, 1999], and H_2O [*Coheur et al.*, 2002; *Fally et al.*, 2003] were included in the fitting procedure as well. To compensate for the filling up of the Fraunhofer lines in the solar spectrum by inelastic scattering, the so-called Ring effect [*Platt and Stutz*, 2008], a synthetic Ring spectrum calculated from a high-resolved solar spectrum (R. L. Kurucz, I. Furenlid, J. Brault, and L. Testerman, 1984, Solar flux atlas from 296 to 1300 nm) (http://kurucz.harvard.edu/sun/fluxatlas/) using the DOASIS software [*Kraus*, 2003] was also included in the fit. Details of every fitting interval and cross sections used are shown in Table 1. Examples of DOAS fits for NO_2, HCHO, and SO_2 are shown in Figure 1. The number of spectra collected for the SO_2 and NO_2 measurements was in all cases automatically adapted to give a time resolution of approximately 5 s per measurement point. However, for HCHO evaluation, spectra were coadded in order to increase the signal-to-noise ratio, resulting in a time resolution of 86 s per measurement point.

2.4. Wind Data

[13] Wind speed and wind direction data were obtained from wind fields recorded by GPS balloon sondes (RS80-15N-V2D-A-GPS) obtained from Environmental Science Corporation, Boulder, Colorado. GPS sondes were launched in between our measurements and nearby the measurement paths used. Typically, three or four balloon sondes were launched every day; the rise speed of the balloons was typically 5 m s^{-1}. In the HSC the soundings were carried out close to the Lynchburg Ferry crossing (Figure 2), and in Texas City the soundings were launched westward of the town (Figure 3). When balloon sondes were not available, wind data were used from a radar profiler operated by the Texas Commission of Environmental Quality within the NOAA profiler network at the La Porte Airport south of the HSC.

[14] The measurements presented in this study were conducted in sunny conditions. Under these conditions the industrial emission plumes mix rather quickly in the vertical, giving a homogeneous distribution of the pollutants versus height through the mixing layer even several kilometers downwind. In addition to the atmospheric mixing, the plumes from process industries exhibit an initial lift since they are usually hotter than the surrounding air. This assumption of rapid mixing agrees with Doppler lidar measurements conducted from the ship RV *Ronald H. Brown* by NOAA during the TexAQS 2006 [*Tucker et al.*, 2009]. From these measurements information about mixing height and the vertical mixing of the atmosphere could be obtained showing typical daytime vertical mixing speeds of ± (0.5–1.5) m s^{-1}.

[15] The measurements presented in this study were typically conducted at a plume transport time of 200–500 s

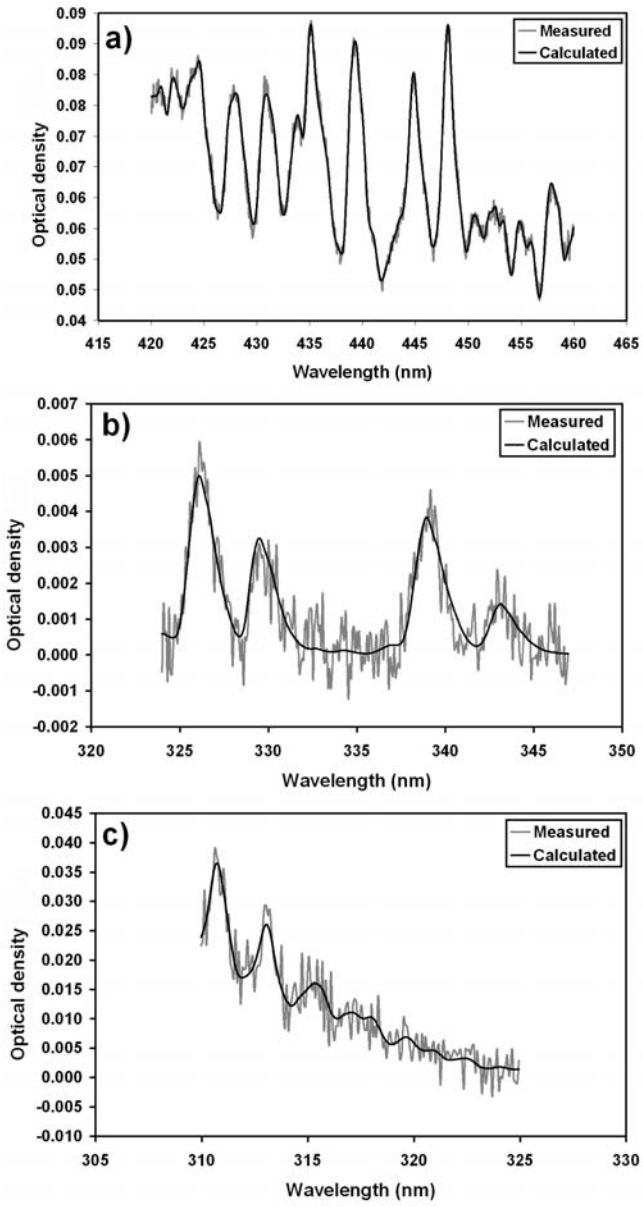

Figure 1. Examples of differential optical absorption spectroscopy (DOAS) fit in different wavelength regions. Fitted cross sections of (a) NO_2 in the wavelength region of 420–460 nm, (b) HCHO in the wavelength region of 324–347 nm, and (c) SO_2 in the wavelength region of 310–325 nm.

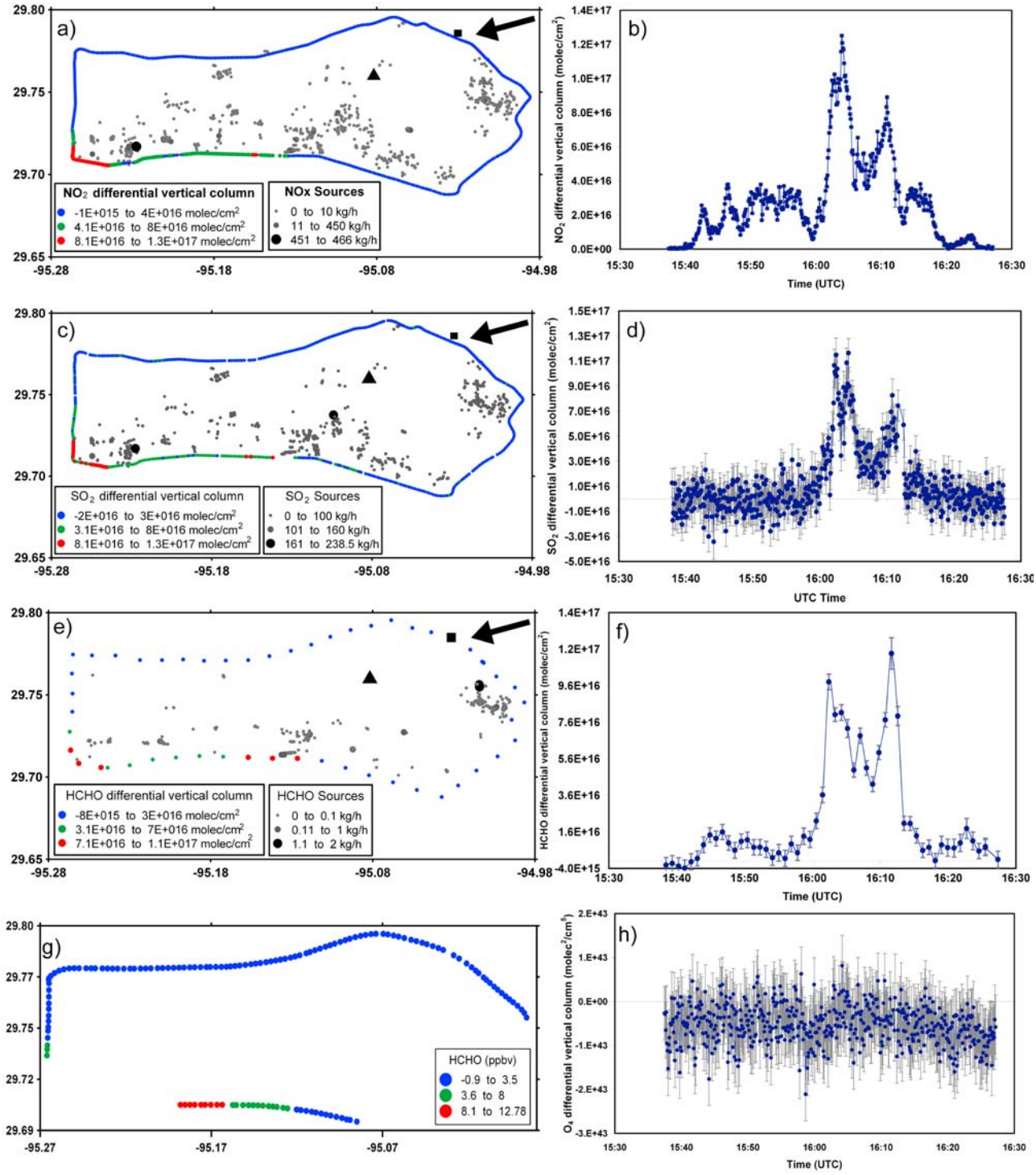

Figure 2. Measurement performed on 31 August 2006 starting at 1037 LT at the Houston Ship Channel. Shown are the spatial distributions of (a) NO_2, (c) SO_2, and (e) HCHO along the Houston Ship Channel quantified during the traverse, the measured differential vertical columns of (b) NO_2, (d) SO_2, and (f) HCHO, (g) the spatial distribution of HCHO measured by the Piper Aztec aircraft, and (h) the differential vertical column of O_4 measured during the traverse. The black square indicates the starting point of the traverse. The site where balloon sondes were launched (close to the Lynchburg Ferry crossing) is indicated by a black triangle. In gray scale, the known NO_x, SO_2, and HCHO sources from the EI in the HSC are shown. The black arrow at the right upper corner of Figures 2a, 2c, and 2e indicates the wind direction obtained from wind fields recorded by a GPS balloon sonde launched at 0953 LT.

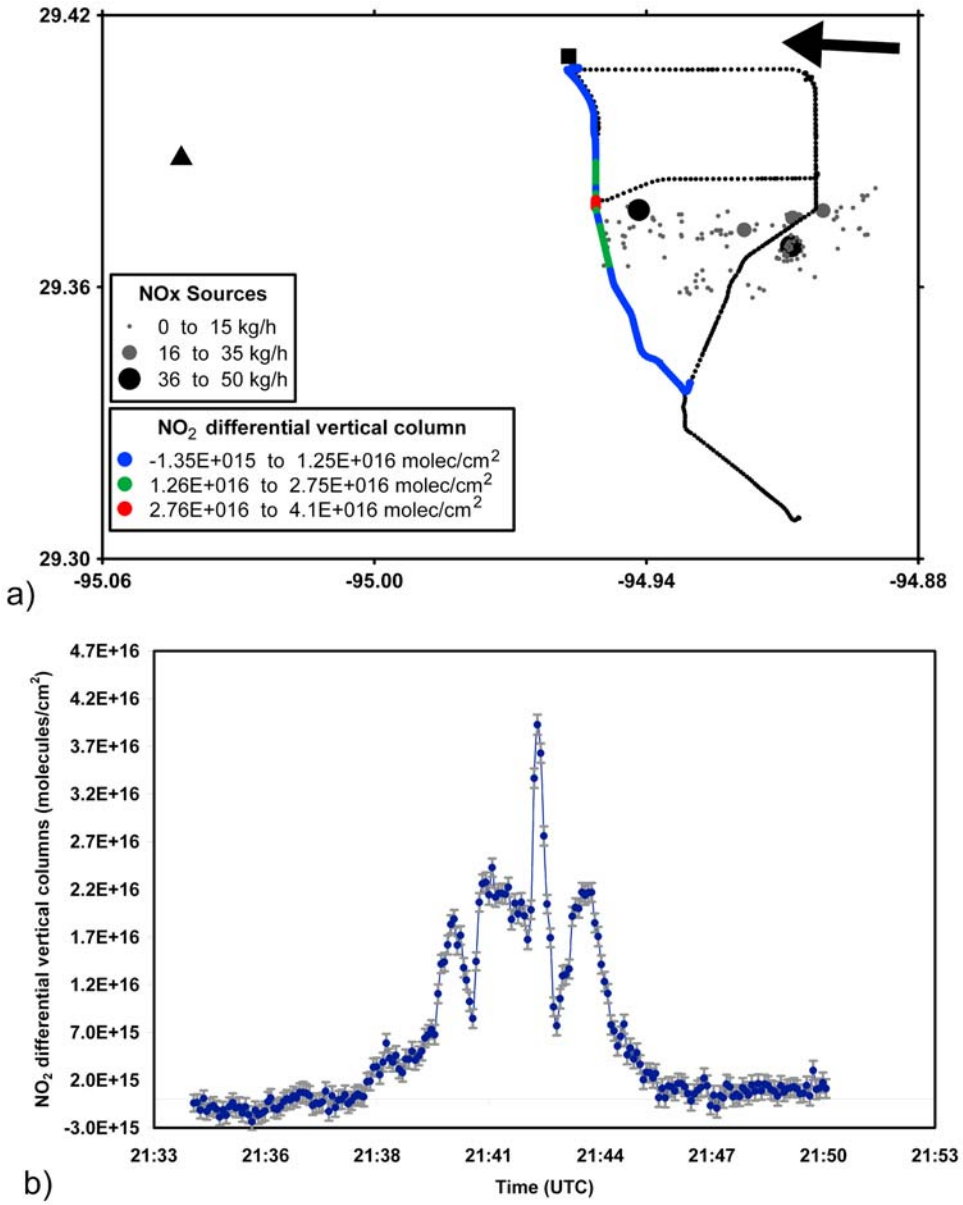

Figure 3. Measurement performed on 20 September 2006 starting at 1634 LT at Texas City. (a) The spatial distribution of NO_2 along the measurement path quantified during the traverse. (b) Measured differential vertical columns of NO_2 along the traverse. The black square indicates the starting point of the traverse. The site where balloon sondes were launched is indicated by a black triangle. In gray scale, the known NO_x sources from the EI in Texas City are shown. The black arrow at the right upper corner of Figure 3a indicates the wind direction obtained from wind fields recorded by a GPS balloon sonde launched at 1428 LT.

downwind of the industries, which, according to the discussion above, means that sufficient time has elapsed for the emission plume to mix at heights of up to several hundred meters above the ground. For this reason we have used the average wind over the lower 500 m of the atmosphere as a proxy for the mass-weighted wind.

2.5. Emission Error Estimation

[16] Several types of errors can affect the calculation of emissions using a miniDOAS instrument. A spectroscopic error is related to errors in the absorption cross sections, temperature changes in the spectrometer, fitting errors, and spectral interferences. The spectroscopic error in this study reflects the error in calculated emissions due to the DOAS retrieval of the differential vertical column and was calculated as 10%, 14%, and 40% for NO_2, HCHO, and SO_2 respectively.

[17] A scattering error is expected due to light path extension inside the plume (multiple scattering) as well as to scattering of photons into the instrument's field of view by particles beneath the plume (light dilution). The scattering error strongly depends on meteorological conditions (i.e., cloud coverage, fog, and rain) [*Millán*, 1980; *Moffat and Millán*, 1971] and changes as a function of the distance of

Table 2. Summary of Total Quantified Fluxes (Median) and Comparison With Emissions Inventory[a]

NO_2		NO_x (kg h^{-1})		SO_2			HCHO		
Flux (kg h^{-1})	No. Meas.	Adjusted Values[b]	EI	Flux (kg h^{-1})	No. Meas.	EI	Flux (kg h^{-1})	No. Meas.	EI
Houston Ship Channel									
2542 (214)	9	3435 (289)	2015	1749 (160)	3	1308	481 (21)	3	14
Texas City									
452 (115)	11	619 (158)	433						

[a]The median absolute deviation from the median is shown in parentheses. Abbreviation is as follows: EI, emission inventory.
[b]The NO_x fluxes have been adjusted from the original quantified total NO_2 values according to the NO_2/NO_x ratio derived by aircraft measurements: 0.74 for Houston Ship Channel and 0.73 for Texas City. NO_x fluxes have no further correction applied for rapid photochemical NO_x loss.

the instrument from the plume and the wavelength region used in the DOAS retrieval, becoming more significant at shorter wavelengths for the case of SO_2 [*Mori et al.*, 2006]. Because the measurements presented in this study were conducted during days of clear blue sky without presence of clouds and care was taken to disregard measurements with clear indication of enhanced light paths during the traverses (see section 2.2), the scattering error was assumed to be 10% for this study.

[18] The main uncertainty, however, is due to assumptions about the vertical distribution of the plume, which will lead to errors in attributing the true wind speed for each molecule in the plume. Because we are not able to calculate the plume height with our measurements, we have assumed that the emission plume from an industry mixes rather quickly vertically, due to convection from solar heating of the ground, with a speed of about 0.5–1.5 m s^{-1} in addition to initial plume lifting due to high temperature. Further discussion about the wind data used in this study can be found in section 2.4 and the paper of *Mellqvist et al.* [2010]. Uncertainty in the wind speed and wind direction from GPS balloon sondes, used to calculate emissions presented in this study, is about 30% [*Mellqvist et al.*, 2010]. Our estimated uncertainty in the wind field accounts for possible measurement errors and systematic spatial wind differences, in addition to errors in estimated plume height and therefore errors in wind speed and wind direction used to calculate fluxes, as well as errors due to changes in wind speed and wind direction during the period of time a measurement is being conducted. Further details about expected errors using this technique are given by *Johansson et al.* [2008] and *Rivera et al.* [2009].

[19] Another uncertainty regarding the measurement method is the fact that the measurements are conducted using a mobile van and driving on roads exposed to traffic emissions. Because in this study it is not possible to separate industrial plumes from traffic emissions, we have assumed that emissions from traffic are negligible compared to emissions by industries and form part of the background emissions.

[20] The combined uncertainty for calculated emissions taking into consideration all errors and uncertainties is therefore 33%, 35%, and 51% for NO_2, HCHO, and SO_2, respectively.

2.6. Airborne Measurements

[21] A Piper Aztec (N6670Y) aircraft operated by the Baylor Institute for Air Science conducted several research tasks during the TexAQS 2006 field experiment. Aircraft-based measurements were focused on the collection of lower tropospheric air quality data from August through October 2006 in the Houston region.

[22] NO, NO_2, HCHO, and reactive alkenes, among other parameters, were measured during the conducted flights. NO and NO_2 data recorded during flights conducted on the same measurement paths as our measurements by the Piper Aztec aircraft were used in this study with the objective to gain knowledge of the NO_2/NO_x ratio. NO was measured using an Eco Physics CLD 77. NO_2 mixing ratios were measured using the photolysis-chemiluminescence technique [*Kley and McFarland*, 1980], consisting of a Thermo Environmental 42C instrument and a Droplet Measurement Technologies BLC photolytic converter. Baseline corrections, from the periodic in-flight zeroing of the instruments, were applied automatically for both species. Corrections for both ambient water and pressure were also applied. The uncertainty of NO and NO_2 was 0.4 and 0.2 ppbv, respectively [*Alvarez et al.*, 2007].

3. Results and Discussion

[23] Measurements were performed between 30 August and 29 September 2006 aimed at quantifying emissions from different areas in the HGA. All measurements were compared with reported values in order to give insight into the consistency of our measurements with the available emission inventories of the area. An emissions inventory (EI) developed by the Texas Commission on Environmental Quality was used in this study (the 2006 Point Source Emissions Inventory) (http://www.tceq.state.tx.us/implementation/air/industei/psei/psei.html). It contains daily averaged emission data for approximately 3000 sources for the time period 15 August to 15 September 2006. During this period, some industrial facilities in the HGA reported their monitored hourly emissions of NO_x, SO_2, and VOCs, among other pollutants. In the EI used, these data have been merged with an annual database, providing daily emissions for sources not included in the hourly monitored data set. It is important to notice that daily emissions reported by the industries show very little variability (about 1%) during the days our measurements were compared with the inventory.

[24] Table 2 shows a comparison between the median of total fluxes measured in this field study and reported emissions in the inventory for HSC and TC sites. The median absolute deviation from the median (MAD) refers to the variability of daily quantified fluxes during the field campaign and not to uncertainty of the measurement itself (discussed in section 2.5). In addition, a detailed account of

Table 3. NO_2, SO_2, and HCHO Quantified Fluxes During the Field Campaign

Date	Start Time (LT)	Species	Wind Direction (°)	Wind Speed (m s^{-1})	Flux (kg h^{-1})
		Houston Ship Channel			
31 Aug 2006	0833	NO_2	75	2.07	2756
	0946	NO_2	75	2.07	2650
		HCHO			542
	1037	NO_2	75	2.07	2540
		SO_2			3493
		HCHO			481
	1153	NO_2	85	2.04	1411
		SO_2			1589
		HCHO			460
4 Sep 2006	1250	NO_2	81	3.64	946
		SO2			1749
19 Sep 2006	1127	NO_2	47	10.78	4075
	1221		31	6.55	2817
	1512		38	4.26	2542
	1604		38	4.26	2402
		Texas City			
2 Sep 2006	1340	NO_2	99	1.51	186
	1405		105	2.23	250
14 Sep 2006	0950	NO_2	102	3.96	452
	1118		102	3.96	449
20 Sep 2006	1012	NO_2	67	6.16	567
	1059		67	6.16	634
	1310		77	4.9	404
	1425		93	3.72	375
	1506		93	3.72	499
	1619		93	3.72	644
	1634		93	3.72	596

daily measurements carried out during the field campaign is presented in Table 3.

3.1. NO_x Emissions

[25] Figure 2a shows the spatial distribution of differential NO_2 columns (color coded) quantified during a measurement conducted at the HSC on 31 August 2006 starting at 1037 LT. The known emission sources from the EI inside the HSC are shown as gray dots. Figure 2b shows the differential NO_2 columns quantified during the measurement. The traverse started at the northeast part of the HSC (black square in Figure 2a) and continued toward the west. Two main peaks were found during the traverse; the highest peak found at the southwest is thought to include most of the accumulated emissions of the HSC, while the second, smaller peak most likely represents emissions from the eastern part of the HSC. As discussed in section 2.2, the oxygen dimer (O_4) was included into the DOAS fit in order to indicate the presence of high aerosol loading, which could lead to enhanced light paths through multiple scattering. Figure 2h shows the differential O_4 columns quantified during the measurement where a stable behavior of the oxygen dimer during the traverse is evident, indicating no enhanced light paths during the traverse.

[26] From NO_2 emissions data reported in Table 3, it can be seen that differences in NO_2 emission rates were found at the HSC during the same day and among different days. On 31 August, NO_2 quantified emissions dropped by half comparing a traverse conducted at 1153 LT to traverses conducted previously during the same day.

[27] Figure 3a shows the spatial distribution of differential NO_2 columns (color coded) quantified during a measurement conducted at TC on 20 September 2006 starting at 1634 LT. The known NO_x emission sources of the TC area are shown as gray dots. Figure 3b shows the differential NO_2 columns quantified during the measurement. The traverse started at the north part of a highway located west of TC (black square in Figure 3a) and continued toward the southeast. A main peak was identified during the traverse, found at the western part of the TC industrial area. This peak is thought to represent one of the largest sources of NO_x in the area located at the western part. The other, smaller peaks most likely represent emissions from the whole TC area in general. Some differences were found in NO_2 quantified emissions at TC among different days (Table 3).

[28] The instrument used in this field campaign is capable of quantifying NO_2 but not NO_x, which is given in the inventories. Knowledge about the ratio NO_2/NO_x becomes important in order to assess the consistency of our measurements with the available inventories. Here we have used data from measurements conducted by the Piper Aztec aircraft flying above the same measurement paths we have used to quantify emissions from the HSC and TC industrial sites. Aircraft-based measurements indicate a NO_2/NO_x ratio of 0.74 for HSC and 0.73 for TC along the measurement paths we have used. Figure 4 shows recorded NO_2 and NO_x mixing ratios by the Piper Aztec aircraft while performing a vertical profile between 356 and 1265 m above mean sea level along the HSC on 31 August 2006 at 0800-0815 LT. As can be seen, most of the quantified NO_x is in the form of NO_2. For this field experiment, NO_x average emissions have been estimated from the original quantified total NO_2 values according to the NO_2/NO_x ratio derived by aircraft measurements: 0.74 for HSC and 0.73 for TC. This ratio was estimated for only 1 day for each industrial area; however, it was extrapolated to other measurement days, slightly adding uncertainty to our emission estimates of NO_x.

[29] In summary, large differences in quantified NO_2 emissions were found during and among different days of the field campaign. Our results show that NO_x-derived emissions from the HSC and TC industrial areas are 70%

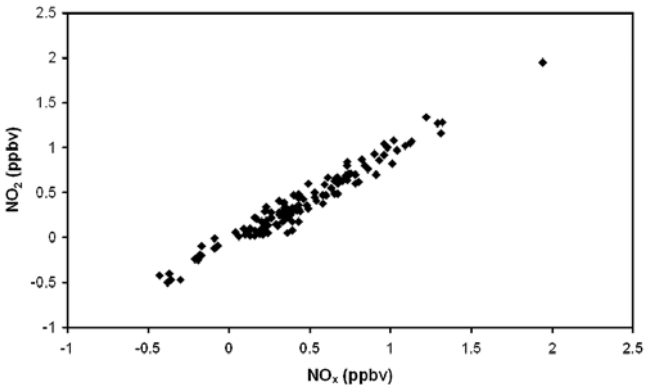

Figure 4. NO_2 and NO_x mixing ratios recorded by the Piper Aztec aircraft while performing a vertical profile between 356 and 1265 m above mean sea level along the Houston Ship Channel on 31 August 2006 at 0800–0815 LT.

and 43%, respectively, above the reported inventory values, with 33% uncertainty.

[30] A study conducted by *Williams et al.* [2009] during the TexAQS 2006 reveals that NO_x emissions from commercial marine shipping in the HGA are significant and present large variability (30%–40% relative standard deviation), which could explain NO_x emissions measured in excess in the HSC and probably to a lesser extent in TC, as well as the measured short-term variability in emissions found at the HSC during the field campaign.

3.2. SO_2 Emissions

[31] During the measurement period, SO_2 plumes were only successfully quantified in the HSC industrial area. Figure 2c shows the spatial distribution of differential SO_2 columns (color coded) quantified during a measurement conducted at the HSC on 31 August 2006 starting at 1037 LT. The known SO_2 emission sources from the EI inside the HSC are shown as gray dots. Figure 2d shows the differential SO_2 columns quantified during the measurement. The traverse started at the northeast part of the HSC (black square in Figure 2c) and continued toward the west. Two main SO_2 peaks were found during the traverse, coinciding with the previously discussed NO_2 peaks. As for the case of NO_2, the highest SO_2 peak found at the southwest is thought to include most of the accumulated emissions of the HSC, while the second, smaller peak most likely represents emissions from the eastern part of the HSC.

[32] Table 2 shows a comparison between measured SO_2 fluxes and reported values in the inventory. The reported daily emissions from the EI are also presented for comparison. In addition, a full summary of daily SO_2 measurements carried out during the field campaign is presented in Table 3. Table 2 indicates that the quantified SO_2 fluxes at the HSC industrial area were 34% higher than the emissions reported in the inventory, with a range of uncertainty, however, that encompasses the inventory.

3.3. HCHO Event

[33] On only 1 day during the field campaign was it possible to clearly identify the presence of HCHO in the plumes from the HGA. On 31 August 2006, HCHO was quantified during three consecutive measurements performed at the HSC industrial site between 0946 and 1245 LT (1446-1745 UTC). Figure 2e shows the spatial distribution of differential HCHO columns (color coded) quantified during a measurement conducted at the HSC on 31 August 2006 starting at 1037 LT. The known HCHO emission sources from the EI inside the HSC are shown as gray dots. Figure 2f shows the differential HCHO columns quantified during the measurement. The traverse started in the northeastern part of the HSC (black square in Figure 2e) and continued toward the west. As for the case of the NO_2 and SO_2 emissions measured during the same traverse, two main HCHO peaks were found during this traverse; the smaller peak found in the southeastern corner is thought to include the accumulated flux of the entire HSC, while the second, larger peak most likely represents the flux from the eastern part of the HSC where most of the HCHO sources are located.

[34] The three consecutive transects yielded a median flux of 481 kg h^{-1} with a MAD of 21 kg h^{-1}. From HCHO fluxes data reported in Table 3, it can be seen that the quantified HCHO fluxes during the three consecutive traverses give very similar values. The high HCHO quantified flux at the HSC is unexpected, especially when compared to the emissions inventory of 14 kg h^{-1} of HCHO for the HSC area (Table 2), representing primary emissions from the industries. It is important to note that only a small fraction of industrial facilities specify, in the data reported in the EI, the type of VOC emitted. In this case we have added all sources located inside the HSC that specifically report HCHO emissions; however, it is possible that some facilities have been missed because of the way of reporting HCHO as VOCs in general.

[35] During the morning flight of 31 August 2006, the Piper Aztec aircraft measured elevated mixing ratios of HCHO over the HSC. Figure 2g shows the spatial distribution of HCHO along the HSC measured by the Piper Aztec aircraft. The peak on the HCHO mixing ratio measured by the aircraft at the southern part of the HSC (Figure 2g) coincides with measurements reported in this study conducted by the mobile miniDOAS instrument.

[36] It is highly likely that the quantified HCHO in the HSC during this field observation was not directly emitted but rather was formed by oxidation of emitted VOCs. During this flight, the Piper Aztec aircraft also measured elevated mixing ratios of reactive alkenes at the southwestern part of the HSC [*Alvarez et al.*, 2007], coinciding with HCHO measurements reported in this study conducted by the mobile miniDOAS instrument. In addition, *Mellqvist et al.* [2007, 2010] measured large and highly variable emissions of propene, 200–2000 kg h^{-1}, on the same day and upwind of the location where the high formaldehyde differential columns were measured with the mobile miniDOAS instrument [*Mellqvist et al.*, 2007]. In addition, 31 August 2006 was characterized by low wind speeds (about 2 m s^{-1}), suggesting both more concentrated VOC levels and a longer photochemical processing time between the VOC emission and sampling time.

[37] We consider that the presence of HCHO in the HSC on 31 August 2006 is an isolated event rather than a permanent situation since it was only observed for a short period of time (3 h) and only once during 5 weeks of measurements conducted in the HGA. The occurrence of industrial emission events in the HGA has been previously identified and studied. They typically last hours to days and are largely made up of ethene and propene. Some events are reported to release a few hundred kilograms [*Murphy and Allen*, 2005], while others have been reported to lead to emission rates of up to several thousand kilograms per hour [*Vizuete et al.*, 2008]. More than half of the mass of highly reactive VOC emission events has been attributed to ethene and almost one third to propene; the remainder consists of isomers of butene and 1,3-butadiene [*Murphy and Allen*, 2005]. In this case, the HCHO quantified in the HSC cannot be regarded as an emission but rather as the photochemical production of HCHO by the oxidation of emitted alkenes, which tend to efficiently produce HCHO [*Dodge*, 1990; *Goldan et al.*, 2000; *Lee et al.*, 1998; *Wert et al.*, 2003].

[38] In addition, as part of the TexAQS 2006 field experiment, *Brooks et al.* [2009] report extreme pollution events in the early morning hours of 31 August 2006 during measurements conducted atop the Moody Tower

TexAQS II Radical Measurement Project site. Their findings include the highest fine particulate mercury value observed on 31 August 2006, along with extremely high values of VOCs, SO_2, aerosol mass, and most other primary pollutants. At 1430 UTC spikes in HCHO (23 ppb), PAN (3.6 ppb), and O_3 (~100 ppb) were reported as well. Back trajectories and wind direction showed air parcels coming from the Houston Ship Channel [*Brooks et al.*, 2009].

4. Conclusions

[39] In summary, measurements conducted during the TexAQS 2006 field experiment show that measured SO_2 emissions at HSC were 34% higher than the emissions reported in the inventory, with a range of uncertainty, however, that encompasses the inventory. The derived NO_x emissions at the HSC and TC industrial areas were 70% and 43%, respectively, above the reported inventory values, with 33% uncertainty. This should be compared to mobile solar infrared measurements and airborne measurements showing an order of magnitude difference in measured and reported ethene emissions from industrial sources in the HGA [*De Gouw et al.*, 2009]. Short-term variability of NO_x and SO_2 emissions were also found. On 31 August 2006, the measured emissions of NO_2 and SO_2 at the HSC dropped by half between a traverse conducted at 1153 LT when compared to traverses conducted previously during the same day.

[40] During the TexAQS 2006 field experiment, it was possible to identify a HCHO event occurring on 31 August 2006 yielding HCHO fluxes an order of magnitude greater than the reported primary emissions in the inventory. For this reason and due to the fact that during daytime, generally the amount of primary emitted HCHO is considerably smaller than the amount that is secondarily photochemically produced [*Wert et al.*, 2003], it is highly likely that the quantified HCHO in the HSC was formed by oxidation of emitted alkenes since these tend to efficiently produce HCHO, implying a very rapid photochemical conversion.

[41] **Acknowledgments.** Funding for this work was provided by Texas Environmental Research Consortium (TERC) under project H53. The authors would like to thank Craig Clements for conducting some of the GPS soundings and John Johansson for estimation of NO_2/NO_x ratios. We thank TCEQ for supplying wind profiler data. The Baylor Piper Aztec data were funded by TERC under project H63. We thank Levi Kauffman, Tim Compton, Grazia Zanin, Maxwell Shauck, and Martin Buhr for conducting part of the work with the Piper Aztec and Noor Gillani for flight planning.

References

Allen, D., C. Murphy, Y. Kimura, W. Vizuete, T. Edgar, H. Jeffries, B. Kim, M. Webster, and M. Symons (2004), Variable industrial VOC emissions and their impact on ozone formation in the Houston Galveston area: Final report on Texas Environmental Research Consortium project H-13, Univ. of Tex., Austin.

Alvarez, S., L. Kauffman, T. Compton, G. Zanin, M. Shauck, and M. Buhr (2007), H-63 aircraft measurements in support of TexAQS II: Project H63 final report, Tex. Environ. Res. Consortium, Houston.

Berkowitz, C. M., C. W. Spicer, and P. V. Doskey (2005), Hydrocarbon observations and ozone production rates in western Houston during the Texas 2000 Air Quality Study, *Atmos. Environ.*, *39*, 3383–3396, doi:10.1016/j.atmosenv.2004.12.007.

Bobrowski, N., and U. Platt (2007), SO_2/BrO rations studied in five volcanic plumes, *J. Volcanol. Geotherm. Res.*, *166*, 147–160, doi:10.1016/j.jvolgeores.2007.07.003.

Bobrowski, N., G. Hönninger, B. Galle, and U. Platt (2003), Detection of bromine monoxide in a volcanic plume, *Nature*, *423*, 273–276, doi:10.1038/nature01625.

Bogumil, K., et al. (2003), Measurements of molecular absorption spectra with the SCIAMACHY pre-flight model: Instrument characterization and reference data for atmospheric remote-sensing in the 230–2380 nm region, *J. Photochem. Photobiol. A Chem.*, *157*, 167–184, doi:10.1016/S1010-6030(03)00062-5.

Brock, C. A., et al. (2003), Particle growth in urban and industrial plumes in Texas, *J. Geophys. Res.*, *108*(D3), 4111, doi:10.1029/2002JD002746.

Brody, S. D., B. M. Peck, and W. E. Highfield (2004), Examining localized patterns of air quality perception in Texas: A spatial and statistical analysis, *Risk Anal.*, *24*, 1561–1574, doi:10.1111/j.0272-4332.2004.00550.x.

Brooks, S., W. Luke, M. Cohen, P. Kelly, B. Lefer, and B. Rappenglück (2009), Mercury species measured atop the Moody Tower TRAMP site, Houston Texas, *Atmos. Environ.*, doi:10.1016/j.atmosenv.2009.02.009.

Buzcu-Guven, B., and M. P. Fraser (2008), Comparison of VOC emissions inventory data with source apportionment results for Houston, TX, *Atmos. Environ.*, *42*, 5032–5043, doi:10.1016/j.atmosenv.2008.02.025.

Byun, D. W., S.-T. Kim, and S.-B. Kim (2007), Evaluation of air quality models for the simulation of a high ozone episode in the Houston metropolitan area, *Atmos. Environ.*, *41*, 837–853, doi:10.1016/j.atmosenv.2006.08.038.

Coheur, P.-F., S. Fally, M. Carleer, C. Clerbaux, R. Colin, A. Jenouvrier, M.-F. Mérienne, C. Hermans, and A. C. Vandaele (2002), New water vapor line parameters in the 26000–13000 cm^{-1} region, *J. Quant. Spectrosc. Radiat. Transfer. 74*, 493–510.

Conley, F. L., R. L. Thomas, and B. L. Wilson (2005), Measurement of volatile organic compounds in the urban atmosphere of Harris County, Texas, *J. Environ. Sci. Health.*, *40*, 1689–1699.

Crutzen, P. (1979), The role of NO and NO_2 in the chemistry of the troposphere and stratosphere, *Annu. Rev. Earth Planet. Sci.*, *7*, 443–472, doi:10.1146/annurev.ea.07.050179.002303.

Daum, P. H., L. I. Kleinman, S. R. Springston, L. J. Nunnermacker, Y.-N. Lee, J. Weinstein-Lloyd, J. Zheng, and C. M. Berkowitz (2003), A comparative study of O_3 formation in the Houston urban and industrial plumes during the 2000 Texas Air Quality Study, *J. Geophys. Res.*, *108*(D23), 4715, doi:10.1029/2003JD003552.

Daum, P. H., L. I. Kleinman, S. R. Springston, L. J. Nunnermacker, Y.-N. Lee, J. Weinstein-Lloyd, J. Zheng, and C. M. Berkowitz (2004), Origin and properties of plumes of high ozone observed during the Texas 2000 Air Quality Study (TexAQS 2000), *J. Geophys. Res.*, *109*, D17306, doi:10.1029/2003JD004311.

De Gouw, J. A., et al. (2009), Airborne measurements of ethene from industrial sources using laser photo-acoustic spectroscopy, *Environ. Sci. Technol.*, *43*, 2437–2442, doi:10.1021/es802701a.

Dodge, M. C. (1990), Formaldehyde production in photochemical smog as predicted by three state-of-the-science chemical oxidant mechanisms, *J. Geophys. Res.*, *95*, 3635–3648, doi:10.1029/JD095iD04p03635.

Fally, S., P.-F. Coheur, M. Carleer, C. Clerbaux, R. Colin, A. Jenouvrier, M.-F. Mérienne, C. Hermans, and A. C. Vandaele (2003), Water vapor line broadening and shifting by air in the 26,000–13,000 cm^{-1} region, *J. Quant. Spectrosc. Radiat. Transf.*, *82*, 119–131.

Finlayson-Pitts, B. J., and J. N. Pitts (2000), *Chemistry of the Upper and Lower Atmosphere: Theory, Experiments and Applications*, Academic, San Diego, Calif.

Galle, B., C. Oppenheimer, A. Geyer, A. J. S. McGonigle, M. Edmonds, and L. Horrocks (2002), A miniaturised ultraviolet spectrometer for remote sensing of SO_2 fluxes: A new tool for volcano surveillance, *J. Volcanol. Geotherm. Res.*, *119*, 241–254, doi:10.1016/S0377-0273(02)00356-6.

Garcia, A. R., R. Volkamer, L. T. Molina, M. J. Molina, J. Samuelsson, J. Mellqvist, B. Galle, S. C. Herndon, and C. E. Kolb (2006), Separation of emitted and photochemical formaldehyde in Mexico City using a statistical analysis and a new pair of gas-phase tracers, *Atmos. Chem. Phys.*, *6*, 4545–4557.

Gilman, J. B., et al. (2009), Measurements of volatile organic compounds during the 2006 TexAQS/GoMACCS campaign: Industrial influences, regional characteristics, and diurnal dependencies of the OH reactivity, *J. Geophys. Res.*, *114*, D00F06, doi:10.1029/2008JD011525.

Goldan, P. D., D. D. Parrish, W. C. Kuster, M. Trainer, S. A. McKeen, J. Holloway, B. T. Jobson, D. T. Sueper, and F. C. Fehsenfeld (2000), Airborne measurements of isoprene, CO, and anthropogenic hydrocarbons and their implications, *J. Geophys. Res.*, *105*, 9091–9105, doi:10.1029/1999JD900429.

Grover, R., and M. L. Bradford (2001), Texas NO_x state implementation plan for Houston-Galveston area, *Environ. Prog.*, *20*, 197–205, doi:10.1002/ep.670200407.

Hermans, C., A. C. Vandaele, M. Carleer, S. Fally, R. Colin, A. Jenouvrier, B. Coquart, and M.-F. Mérienne (1999), Absorption cross-sections of atmospheric constituents: NO_2, O_2, and H_2O, *Environ. Sci. Pollut. Res.*, *6*, 151–158, doi:10.1007/BF02987620.

Jacob, D. J., et al. (1996), Origin of ozone and NO_x in the tropical troposphere: A photochemical analysis of aircraft observations over the South Atlantic basin, *J. Geophys. Res.*, *101*, 24,235–24,250, doi:10.1029/96JD00336.

Jobson, B. T., C. M. Berkowitz, W. C. Kuster, P. D. Goldan, E. J. Williams, F. C. Fehsenfeld, E. C. Apel, T. Karl, W. A. Lonneman, and D. Riemer (2004), Hydrocarbon source signatures in Houston, Texas: Influence of the petrochemical industry, *J. Geophys. Res.*, *109*, D24305, doi:10.1029/2004JD004887.

Johansson, M., and Y. Zhang (2004), Mobile DOAS, version 4.1, Opt. Remote Sens. Group Chalmers Univ. of Technol., Göteborg, Sweden.

Johansson, M., B. Galle, T. Yu, L. Tang, D. Chen, H. Li, J. X. Li, and Y. Zhang (2008), Quantification of total emission of air pollutants from Beijing using mobile mini-DOAS, *Atmos. Environ.*, *42*, 6926–6933, doi:10.1016/j.atmosenv.2008.05.025.

Johansson, M., C. Rivera, B. de Foy, W. Lei, J. Song, Y. Zhang, B. Galle, and L. Molina (2009), Mobile mini-DOAS measurement of the outflow of NO_2 and HCHO from Mexico City, *Atmos. Chem. Phys.*, *9*, 5647–5653.

Kasibhatla, P. S., H. Levy, W. J. Moxim, and W. L. Chameides (1991), The relative impact of stratospheric photochemical production on tropospheric NO_y levels: A model study, *J. Geophys. Res.*, *96*, 18,631–18,646, doi:10.1029/91JD01665.

Kleinman, L. I., P. H. Daum, D. Imre, Y. N. Lee, L. J. Nunnermacker, S. R. Springston, J. Weinstein-Lloyd, and J. Rudolph (2002), Ozone production rate and hydrocarbon reactivity in 5 urban areas: A cause of high ozone concentration in Houston, *Geophys. Res. Lett.*, *29*(10), 1467, doi:10.1029/2001GL014569.

Kley, D., and M. McFarland (1980), Chemiluminescence detector for NO and NO_2, *Atmos. Technol.*, *12*, 63–69.

Kraus, S. (2003), DOAIS intelligent system, Inst. of Environ. Phys. Univ. of Heidelberg, Germany.

Lee, Y.-N., et al. (1998), Atmospheric chemistry and distribution of formaldehyde and several multioxygenated carbonyl compounds during the 1995 Nashville/Middle Tennessee Ozone Study, *J. Geophys. Res.*, *103*, 22,449–22,462, doi:10.1029/98JD01251.

Lei, W., R. Zhang, X. Tie, and P. Hess (2004), Chemical characterization of ozone formation in the Houston-Galveston area: A chemical transport model study, *J. Geophys. Res.*, *109*, D12301, doi:10.1029/2003JD004219.

Leuchner, M., and B. Rappenglück (2010), VOC source-receptor relationships in Houston during TexAQS-II, *Atmos. Environ.*, in press.

Martin, R. V., et al. (2002), An improved retrieval of tropospheric nitrogen dioxide from GOME, *J. Geophys. Res.*, *107*(D20), 4437, doi:10.1029/2001JD001027.

McGonigle, A. J. S., C. L. Thomson, V. I. Tsanev, and C. Oppenheimer (2004), A simple technique for measuring power station SO_2 and NO_2 emissions, *Atmos. Environ.*, *38*, 21–25, doi:10.1016/j.atmosenv.2003.09.048.

Meller, R., and G. K. Moortgat (2000), Temperature dependence of the absorption cross sections of formaldehyde between 223 and 323 K in the wavelength range 225–375 nm, *J. Geophys. Res.*, *105*, 7089–7101, doi:10.1029/1999JD901074.

Mellqvist, J., J. Samuelsson, C. Rivera, B. Lefer, and M. Patel (2007), Measurements of industrial emissions of VOCs, NH_3, NO_2 and SO_2 in Texas using the solar occultation flux method and mobile DOAS: Project H053.2005, Tex. Environ. Res. Consortium, Houston.

Mellqvist, J., J. Samuelsson, J. Johanssson, C. Rivera, B. Lefer, S. Alvarez, and J. Jolly (2010), Measurements of industrial emissions of alkenes in Texas using the solar occultation flux method, *J. Geophys. Res.*, *115*, D00F17, doi:10.1029/2008JD011682.

Millán, M. M. (1980), Remote sensing of air pollutants. A study of some atmospheric scattering effects, *Atmos. Environ.*, *14*, 1241–1253, doi:10.1016/0004-6981(80)90226-7.

Moffat, A. J., and M. M. Millán (1971), The application of optical correlation techniques to the remote sensing of SO_2 plumes using skylight, *Atmos. Environ.*, *5*, 677–690, doi:10.1016/0004-6981(71)90125-9.

Mori, T., T. Mori, K. Kazahaya, M. Ohwada, J. Hirabayashi, and S. Yoshikawa (2006), Effect of UV scattering on SO_2 emission rate measurements, *Geophys. Res. Lett.*, *33*, L17315, doi:10.1029/2006GL026285.

Murphy, C. F., and D. T. Allen (2005), Hydrocarbon emissions from industrial release events in the Houston-Galveston area and their impact on ozone formation, *Atmos. Environ.*, *39*, 3785–3798, doi:10.1016/j.atmosenv.2005.02.051.

Murphy, D., D. Fahey, M. Proffitt, S. Liu, C. Eubank, S. Kawa, and K. Kelly (1993), Reactive odd nitrogen and its correlation with ozone in the lower stratosphere and upper troposphere, *J. Geophys. Res.*, *98*, 8751–8773, doi:10.1029/92JD00681.

Penner, J. E., C. S. Atherton, J. Dignon, S. J. Ghan, J. J. Walton, and S. Hameed (1991), Tropospheric nitrogen: A three-dimensional study of sources, distributions, and deposition, *J. Geophys. Res.*, *96*, 959–990, doi:10.1029/90JD02228.

Platt, U. (1994), Differential optical absorption spectroscopy (DOAS), in *Air Monitoring by Spectroscopy Techniques*, edited by M. W. Sigrist, pp. 27–83, Wiley-Interscience, New York.

Platt, U., and J. Stutz (2008), *Differential Optical Absorption Spectroscopy: Principles and Applications (Physics of Earth and Space Environments)*, Springer, Berlin, Germany.

Platt, U., D. Perner, and H. W. Pätz (1979), Simultaneous measurement of atmospheric CH_2O, O_3 and NO_2 by differential optical absorption, *J. Geophys. Res.*, *84*, 6329–6335, doi:10.1029/JC084iC10p06329.

Rivera, C., J. A. Garcia, B. Galle, L. Alonso, Y. Zhang, M. Johansson, M. Matabuena, and G. Gangoiti (2009), Validation of optical remote sensing measurement strategies applied to industrial gas emissions, *Int. J. Remote Sens.*, *30*, 3191–3204, doi:10.1080/01431160802558808.

Ryerson, T. B., et al. (2003), Effect of petrochemical industrial emissions of reactive alkenes and NO_x on tropospheric ozone formation in Houston, Texas, *J. Geophys. Res.*, *108*(D8), 4249, doi:10.1029/2002JD003070.

Sinreich, R., U. Friess, T. Wagner, and U. Platt (2005), Multi axis differential optical absorption spectroscopy (MAX-DOAS) of gas and aerosol distributions, *Faraday Discuss.*, *130*, 153–164, doi:10.1039/b419274p.

Smith, L. A., T. H. Stock, K. C. Chung, S. Mukerjee, X. L. Liao, C. Stallings, and M. Afshar (2007), Spatial analysis of volatile organic compounds from a community-based air toxics monitoring network in Deer Park, Texas, USA, *Environ. Monit. Assess.*, *128*, 369–379, doi:10.1007/s10661-006-9320-8.

Tucker, S. C., W. A. Brewer, R. M. Banta, C. J. Senff, S. P. Sandberg, D. C. Law, A. Weickmann, and R. M. Hardesty (2009), Doppler lidar estimation of mixing height using turbulence, shear, and aerosol profiles, *J. Atmos. Oceanic Technol.*, *26*, 673–688, doi:10.1175/2008JTECHA1157.1.

Vandaele, A. C., C. Hermans, P. C. Simon, M. Carleer, R. Colin, S. Fally, M. F. Mérienne, A. Jenouvrier, and B. Coquart (1998), Measurements of the NO_2 absorption cross-section from 42 000 cm^{-1} to 10 000 cm^{-1} (238–1000 nm) at 220 K and 294 K, *J. Quant. Spectrosc. Radiat. Transf.*, *59*, 171–184, doi:10.1016/S0022-4073(97)00168-4.

Van Roozendael, M., and C. Fayt (2001), WinDOAS, version 2.1, Belg. Inst. For Space Aeronomy, Uccle.

Vizuete, W., B.-U. Kim, H. Jeffries, Y. Kimura, D. T. Allen, M.-A. Kioumourtzoglou, L. Biton, and B. Henderson (2008), Modeling ozone formation from industrial emission events in Houston, Texas, *Atmos. Environ.*, *42*, 7641–7650, doi:10.1016/j.atmosenv.2008.05.063.

Voigt, S., J. Orphal, K. Bogumil, and J. P. Burrows (2001), The temperature dependence (203–293 K) of the absorption cross sections of O_3 in the 230–850 nm region measured by Fourier-transform spectroscopy, *J. Photochem. Photobiol. A Chem.*, *143*, 1–9, doi:10.1016/S1010-6030(01)00480-4.

Wert, B. P., et al. (2003), Signatures of terminal alkene oxidation in airborne formaldehyde measurements during TexAQS 2000, *J. Geophys. Res.*, *108*(D3), 4104, doi:10.1029/2002JD002502.

Williams, E. J., B. M. Lerner, P. C. Murphy, S. C. Herndon, and M. S. Zahniser (2009), Emissions of NO_x, SO_2, CO, and HCHO from commercial marine shipping during Texas Air Quality Study (TexAQS) 2006, *J. Geophys. Res.*, *114*, D21306, doi:10.1029/2009JD012094.

Xie, Y., and C. M. Berkowitz (2007), The use of conditional probability functions and potential source contribution functions to identify source regions and advection pathways of hydrocarbon emissions in Houston, Texas, *Atmos. Environ.*, *41*, 5831–5847, doi:10.1016/j.atmosenv.2007.03.049.

S. Alvarez, Institute for Air Science, Baylor University, Waco, TX 76798, USA.

B. Lefer and M. R. Patel, Department of Geosciences, University of Houston, Houston, TX 77004, USA.

J. Mellqvist, C. Rivera, and J. Samuelsson, Radio and Space Science, Chalmers University of Technology, SE-412 96 Gothenburg, Sweden. (claudia.rivera@chalmers.se)